Article

pubs.acs.org/Biomac

Dual Thermosensitive Hydrogels Assembled from the Conserved C-Terminal Domain of Spider Dragline Silk

Zhi-Gang Qian,[†] Ming-Liang Zhou,[†] Wen-Wen Song, and Xiao-Xia Xia*

State Key Laboratory of Microbial Metabolism, Joint International Research Laboratory of Metabolic & Developmental Sciences, and School of Life Sciences and Biotechnology, Shanghai Jiao Tong University, 800 Dongchuan Road, Shanghai 200240, P. R. China

Supporting Information

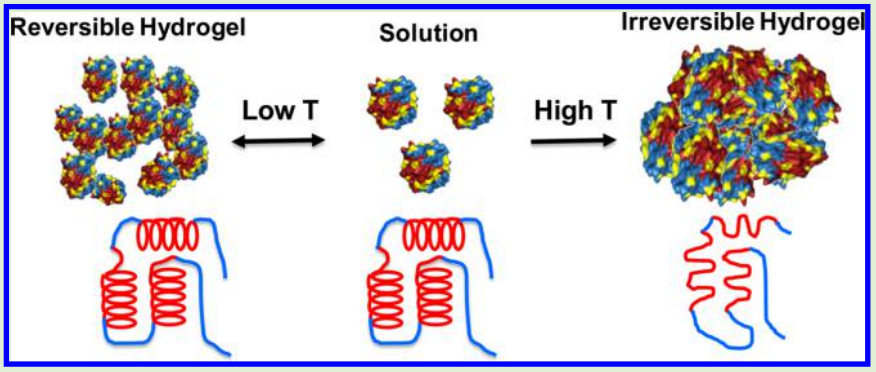

ABSTRACT: Stimuli-responsive hydrogels have great potentials in biomedical and biotechnological applications. Due to the advantages of precise control over molecular weight and being biodegradable, protein-based hydrogels and their applications have been extensively studied. However, protein hydrogels with dual thermosensitive properties are rarely reported. Here we present the first report of dual thermosensitive hydrogels assembled from the conserved C-terminal domain of spider dragline silk. First, we found that recombinant C-terminal domain of major ampullate spidroin 1 (MaSp1) of the spider *Nephila clavipes* formed hydrogels when cooled to approximately 2 °C or heated to 65 °C. The conformational changes and self-assembly of the recombinant protein were studied to understand the mechanism of the gelation processes using multiple methods. It was proposed that the gelation in the low-temperature regime was dominated by hydrogen bonding and hydrophobic interaction between folded protein molecules, whereas the gelation in the high-temperature regime was due to cross-linking of the exposed hydrophobic patches resulting from partial unfolding of the protein upon heating. More interestingly, genetic fusion of the C-terminal domain to a short repetitive region of *N. clavipes* MaSp1 resulted in a chimeric protein that formed a hydrogel with significantly improved mechanical properties at low temperatures between 2 and 10 °C. Furthermore, the formation of similar hydrogels was observed for the recombinant C-terminal domains of dragline silk of different spider species, thus demonstrating the conserved ability to form dual thermosensitive hydrogels. These findings may be useful in the design and construction of novel protein hydrogels with tunable multiple thermosensitivity for applications in the future.

INTRODUCTION

Spider dragline silk, one of the most remarkable biomaterials, is primarily composed of two proteins, major ampullate spidroins 1 (MaSp1) and 2 (MaSp2).[1,2] These spidroins are highly modular, each with a long repetitive sequence that is flanked on both sides by nonrepetitive N-terminal (NT) and C-terminal domains (CT) of approximately 100 amino acids.[3] The nonrepetitive terminal domains are evolutionarily conserved among different spider species and various types of spidroins.[4] The two terminal domains expose a well-structured shape in solution compared to the loose repetitive region of spidroins.[5,6] Previously, much has been done to reveal the structures of the two domains and their roles in silk fiber assembly.[7−11] In particular, the structure of the CT of spider *Araneus diadematus* fibroin 3 has been solved by nuclear magnetic resonance spectroscopy, revealing a five α-helix bundle fold that pair-up permanently in a parallel manner.[7] The homodimeric barrel-like structure is favored by an intermolecular disulfide bond and two pairs of oppositely charged residues that form intramolecular salt bridges.[8] With respect to the primary amino acid sequence, the CT is more hydrophobic than the NT and the repetitive core of a spidroin.[7,11] Nonetheless, the native fold of the CT ensures that the hydrophobic amino acids are buried in a core, while hydrophilic residues such as glutamine and serine are exposed toward the solvent and ensure solubility of the protein.[7] Furthermore, the structural response of the CT to physicochemical variations found in a spider spinning duct is essential for the controlled switching between storage of the soluble spidroin and assembly into an insoluble fiber.[10]

Received: September 14, 2015
Revised: October 7, 2015
Published: October 12, 2015

DOI: 10.1021/acs.biomac.5b01231
Biomacromolecules 2015, 16, 3704−3711

Structural conversions of the CT in response to variations in ionic composition and concentration, pH, and shear forces are known to some extent.[7,12−14] For example, the type of ions encountered, whether Na^+, K^+, Cl^-, or PO_4^{3-}, appears to be a major parameter that influences the structural stability of the CT.[7] On the other hand, shear affects viscosity of solutions of silk-like proteins incorporating the CT and accelerates the aggregation rate of the silk-like proteins.[6,14] In addition, the CT structure is very sensitive to pH and a molten globule state occurs at pH 5.0 and below.[11] Collectively, previous results proved that the CT structure was sensitive to the changing environmental conditions that are physiologically relevant during the silk spinning process. We anticipate that the CT structure may be sensitive to other physiochemical stimuli that remain yet to be identified, and the responsiveness behavior could be potentially applied for the fabrication of novel smart biomaterials.

Responsive hydrogels capable of sensing and responding to external stimuli such as temperature, pH, light, etc. have emerged as an important class of materials for many applications in biotechnology and medicine.[15−17] At present these hydrogels are mainly prepared from a limited number of natural and synthetic polymers.[18,19] More recently, genetically engineered protein-based materials that mimic the remarkable designs in nature have attracted much attention and are continuing to be developed into new alternative materials with various responsive properties. For example, elastin-like protein polymers have been designed to be sensitive to various stimuli including temperature, pH and light and fabricated into a variety of smart biomaterials.[20−22] Resilin-mimetic proteins are another class of interesting protein polymers, which have been reported to be temperature, pH, and photoresponsive with tunable photophysical properties.[23,24] In addition, some unique peptide motifs like coiled coil motifs, β-sheet forming peptides derived from native proteins, have been rationally designed and characterized for the preparation of smart materials.[25−27] Among these smart materials, thermoresponsive hydrogels are one of the most widely studied responsive systems.[28] These systems undergo a phase separation as the temperature is either raised to a critical value known as the lower critical solution temperature (LCST) or decreased to a critical value known as the upper critical solution temperature (UCST). However, dual phase transition behavior (the occurrence of both UCST and LCST) is not common.[29−32] Very few protein polymers such as resilin-mimetic protein and abductin-based protein exhibit thermally induced micelle−unimer−micelle transitions in aqueous solutions.[24,33] As for hydrogels, thermally induced sequential gel−sol−gel transition has not yet been known.

In this study, we report for the first time that the conserved CT of spider dragline silk formed a reversible hydrogel at low temperature and an irreversible hydrogel at high temperature, representing a thermally induced sequential gel−sol−gel transition. The mechanism of the gelation processes at dual temperatures was explored using various methods including circular dichroism, fluorescence spectroscopy, and atomic force microscopy. In addition, we examined whether the CT could help short repetitive units of silk spidroin assemble into hydrogels.

MATERIALS AND METHODS

Strains and Growth Condition. *Escherichia coli* DH5α and BL21 Star(DE3) were obtained from Invitrogen (Life Technologies Corp., Carlsbad, CA) and used for general gene cloning and protein expression, respectively. Bacterial cells were routinely grown at 37 °C in Luria−Bertani (LB) medium (per liter: 10 g tryptone, 5 g yeast extract, 10 g NaCl) supplemented with 50 μg/mL of ampicillin when necessary. Cell growth was monitored by measuring the absorbance at 600 nm (OD_{600}) with a BioPhotometer plus spectrophotometer (Eppendorf, Hamburg, Germany).

Construction of Recombinant Plasmids. All molecular biology procedures were conducted according to standard protocols. All the restriction enzymes and T4 DNA ligase were purchased from New England Biolabs (Ipswich, MA). Plasmid DNA was extracted using the TIANprep Mini Plasmid Kit (TIANGEN Biotech Co., Beijing, China) following the manufacture's protocol.

A synthetic gene encoding the 110 amino-acid CT of *Nephila clavipes* MaSp1 (GenBank accession no. U20329; ref 34) was codon-optimized and flanked by an *Nhe*I restriction site on the 5′ end and a *Spe*I site on the 3′ end. The synthetic gene was synthesized, cloned into *Eco*RV site of vector pUC57, and delivered on plasmid pUC57-MaSpIC from GenScript (Nanjing, China). The synthetic gene was then PCR amplified from pUC57-MaSpIC with primers FcNde (5′-AATCATATGGTGGGCAGCGGCGCGAGC-3′) and RcXho (5′-AATCTCGAGGCCCAGCGCCTGATACACG-3′). The PCR product was digested with restriction enzymes *Nde*I and *Xho*I, agarose gel purified, and cloned into the expression vector pET-19b (Novagen Inc., Madison, WI) at the same sites. The resulting plasmid was named pET19b-NcCT, which permits recombinant expression of the CT of *N. clavipes* MaSp1 with a decahistidine affinity tag under the strong T7 promoter (Figure 1). Likewise, synthetic genes were designed that

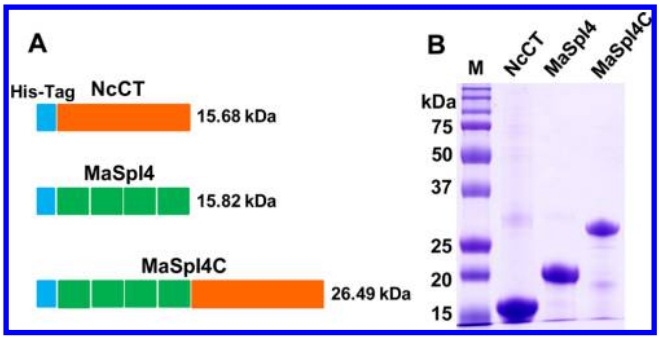

Figure 1. (A) Design of the recombinant proteins. Symbols: blue box, a decahistidine tag; orange box, the C-terminal domain of *N. clavipes* MaSp1; and green box, one repetitive segment of *N. clavipes* MaSp1. The theoretical molecular weights of the recombinant proteins were calculated using the ProtParam tool (http://web.expasy.org/protparam/). (B) SDS−PAGE analysis of the proteins, as labeled above the lanes.

encode the respective CTs of spider *Araneus diadematus* fibroin 3 (GenBank accession no. U47855) and *Euprosthenops australis* MaSp1 (GenBank accession no. AJ973155). For their recombinant expression, plasmids pET19b-AdCT and pET19b-EaCT were constructed.

DNA sequence was designed to encode one repeat of the MaSp1 consensus sequence from *N. clavipes*: GRGGLGGQGAGAAAA-AGGAGQGGYGGLGSQG.[1] The monomer DNA sequence, flanked by restriction sites *Nde*I and *Nhe*I on the 5′ end and *Spe*I and *Xho*I on the 3′ end, was delivered as plasmid pUC57-MaSpI from GenScript. The monomer DNA sequence was then liberated by double digest with *Nde*I and *Xho*I, and cloned into the *Nde*I-*Xho*I site of vector pET-19b (Novagen), leading to plasmid pET19b-MaSpI1. To express two repeats of the MaSp1 consensus sequence, plasmid pET19b-MaSpI2 was constructed by ligating the 1.1-kb, *Pvu*I-*Nhe*I fragment of pET19b-MaSpI1 to the 4.9-kb, *Spe*I-*Pvu*I fragment of pET19b-MaSpI1. Likewise, plasmid pET19b-MaSpI4 was created, which allowed synthesis of the recombinant silk protein having 4 repetitive units of MaSp1.

To express four repetitive units linked with the CT of *N. clavipes* MaSp1, plasmid pET19b-MaSpI4C was constructed by ligating the

DOI: 10.1021/acs.biomac.5b01231
Biomacromolecules 2015, 16, 3704−3711

336-bp, *Nhe*I-*Spe*I fragment of pUC57-MaSpIC with the *Spe*I and alkaline phosphatase treated-plasmid pET19b-MaSpI4. These expression plasmids were identified by restriction digest analysis and confirmed by dideoxy sequencing with both forward and reverse primers based on the T7 promoter and terminator sequences.

Recombinant Protein Expression and Purification. Competent cells of *E. coli* BL21 Star(DE3), a common expression host for pET expression system, were transformed with one of the expression plasmids and plated on selective LB agar plates. A single colony was inoculated into a 15 mL tube containing 4 mL of LB medium and cultured overnight at 37 °C and 220 rpm in the New Brunswick Innova 44R incubator (Eppendorf). One milliliter of the overnight culture was transferred into a 250 mL shake flask containing 100 mL of LB medium. This seed culture, after cultivation for 4 h to reach an OD_{600} of ∼3−4, was then transferred into a 2 L baffled flask containing 800 mL of the Terrific broth (per liter: 12 g of tryptone, 24 g of yeast extract, 5 g of glycerol, 2.31 g of KH_2PO_4, and 12.54 g of K_2HPO_4). The cultures were incubated for ∼6 h and then induced overnight at 16 °C with isopropyl-β-D-thiogalactopyranoside (IPTG) at 1 mM. Cells were harvested by centrifugation at 9000*g* for 15 min at 10 °C. The supernatant was decanted, and the cell pellets were resuspended in a buffer containing 20 mM Tris-HCl (pH 8.0) and 300 mM NaCl, and sonicated with an Ultrasonic Homogenizer (Model JY98-IIIN, Scientz, Ningbo, China). The homogenate was centrifuged at 9000*g* for 10 min at 10 °C. The resulting supernatant was loaded onto a nickel chelating resin column that had been equilibrated with the Tris-HCl buffer (pH 8.0) containing 300 mM NaCl. The column was washed and eluted with the equilibration buffer supplemented with imidazole at 50 mM and 250 mM, respectively. The eluted proteins of interest were changed into 20 mM phosphate buffer (pH 7.2) and concentrated through ultrafiltration using Amicon Ultra centrifugal filters (Millipore, Billerica, MA) at room temperature. The purity of the purified proteins was analyzed by 12% sodium dodecyl sulfate polyacrylamide gel electrophoresis (SDS-PAGE). The protein concentrations were measured using a Pierce BCA Protein Assay Kit (Product No. 23225; Thermo Scientific, Rockford, IL). All the protein samples were freshly prepared before use and maintained in the phosphate buffer (pH 7.2) unless otherwise specified. The molecular weights of the purified proteins were verified by Fourier transform ion cyclotron resonance mass spectrometry (FTICR-MS) on a SolariX-70FT-MS Bruker spectrometer (Bruker Daltonics Inc., Billerica, MA).

Hydrogel Formation. The purified recombinant proteins were prepared with 20 mM phosphate buffer (pH 7.2) to 15% (w/v) at room temperature. Each protein solution (150 μL) was transferred into a glass tube, and precooled to 2 °C. The tubes were incubated at 2 °C for additional 10 min and inversed to evaluate the formation of a self-supporting hydrogel. Images were quickly collected using a Canon EOS 550D digital camera (Canon, Tokyo, Japan). Similarly, incubation and inversion tests were performed at increasing temperatures from 10 to 85 °C, followed by decreasing temperatures from 85 to 2 °C.

Rheological Measurements. Rheological measurements of the protein samples were performed on a stress-controlled AR-G2 rheometer (TA Instruments, New Castle, DE) with a 40 mm diameter plate-on-plate geometry. Freshly prepared protein solutions (400 μL) at 20% (w/v) were loaded onto the preconditioned bottom plate at 25 °C. The top plate was then lowered to a gap distance of 300 μm. Hydrogenated silicone oil was added around the circumference of the geometry to prevent dehydration. The protein samples were first equilibrated at 3.5 °C for 15 min before data collection. The measurements were performed at temperatures ranging from 3.5 to 85 °C with a heating rate of 2 °C/min.

Circular Dichroism (CD). CD spectra were recorded with a Jasco J-815 spectropolarimeter equipped with a Jasco PTC-432S Peltier temperature controller (Tokyo, Japan). Spectra were collected from 190 to 260 nm at a resolution of 0.5 nm by using a 1 mm path length cuvette and a scanning speed of 50 nm/min. Protein solutions (0.5 mg/mL in 20 mM phosphate buffer, pH 7.2) were equilibrated at the indicated temperatures for 5 min before measurements. The CD spectra represented the average of three measurements and were smoothed by using the GraphPad Prism 5 software (GraphPad Software Inc., San Diego, CA). CD data were reported as mean residue ellipticity ($[\theta]$, deg cm^2 dmol^{-1}).[35]

Fluorescence Spectroscopy. Fluorescence measurements were performed using a Hitachi F-7000 fluorescence spectrophotometer (Hitachi, Tokyo, Japan) equipped with a water-circulator cooled cell jacket. Briefly, 1-anilinonaphthalene-8-sulfonic acid (1,8-ANS) was used as the hydrophobic fluorescent probe as previously reported.[36] Freshly prepared proteins and 1,8-ANS (8 mM) were mixed together at a final concentration of 1 mg/mL for the proteins and 80 μM for 1,8-ANS. The mixtures were incubated at 4, 25, or 65 °C for 10 min, respectively, before each measurement. Emission spectra were obtained from wavelength 400 to 600 nm at an excitation wavelength of 370 nm. The fluorescence intensity was analyzed by using the Origin 9.0 software (OriginLab Corp., Northampton, MA).

Atomic Force Microscopy (AFM). AFM was performed in tapping mode using a multimode AFM (Bruker, Germany) with a Nanoscope IIIa scanning probe controller (Digital Instruments, Santa Barbara, CA). The commercial silicon tip probe had a spring constant of ∼3 N/m, and the scan rate was 2 Hz. The AFM images were recorded with 512 × 512 data points. Twenty microliters of the protein samples (1 mg/mL) were casted on mica surfaces at indicated temperatures and allowed to dry for ∼2 days. The AFM images were analyzed using the Nanoscope analysis v5.30 software (Bruker Daltonics Inc., Fremont, CA).

Scanning Electron Microscopy (SEM). The appropriate protein solutions (15%, w/v) were allowed to form hydrogels upon cooling to 4 °C or heating to 65 °C for at least 2 h. The hydrogels were then freeze-dried on a Labconco Freezone 6 Plus lyophilizer (Kansas City, MO). Next, the specimens were coated with gold using a Leica EM SCD050 sputtering device with a water-cooled sputter head (Leica Microsystems GmbH, Vienna, Austria). SEM experiments were then performed on a Hitachi S-3400N scanning electron microscope.

RESULTS AND DISCUSSION

Recombinant Protein Expression and Purification. An earlier study reported the partial cDNA sequence encoding the major ampullate spidroin 1 (MaSp1) of the spider *N. clavipes*.[1] Based on the published sequence (GenBank accession no. U20329), a synthetic gene encoding the 110-amino acid CT of *N. clavipes* MaSp1 was codon optimized and cloned into an expression vector of bacterium *E. coli*. The recombinant CT of *N. clavipes* MaSp1 was designated as NcCT. A silk-like protein, MaSpI4, was designed to have four units of the repetitive consensus sequence of *N. clavipes* MaSp1, which is approximately equal to NcCT regarding theoretical molecule weight (Figure 1A). In addition, a chimeric protein, MaSpI4C, was designed by genetic fusion of the CT to the four units of the repetitive sequence of *N. clavipes* MaSp1.

The recombinant proteins were expressed as decahistidine-tagged fusion proteins and purified under nondenaturing conditions using immobilized metal ion affinity chromatography (IMAC). On denaturing SDS-PAGE gels, the purified NcCT and MaSpI4C appeared as monomers and migrated to the positions as one would expect based on their theoretical molar mass (Figure 1B). Mass spectrometry analysis of NcCT and MaSpI4C revealed molar masses within 0.8% of the expected values of their respective homodimers (Figure S1), indicating that these two proteins existed as homodimers under native conditions. The dimeric feature was in agreement with those previously observed for recombinant CTs of *N. clavipes* MaSp1 (ref 11) and *A. diadematus* fibroin 3 (ref 7). The molecular weight of MaSpI4 was confirmed by mass spectrometry, although this protein migrated to a moderately higher position than expected from its theoretical molar mass of ∼15.8 kDa.

DOI: 10.1021/acs.biomac.5b01231
Biomacromolecules 2015, 16, 3704−3711

Temperature Induced Hydrogel Formation. To test for hydrogel formation, solutions of the recombinant proteins at a concentration of 15% (w/v) in phosphate buffer (pH 7.2) were incubated for 10 min at increasing temperatures from 2 to 85 °C (Figure 2). Interestingly, NcCT formed a transparent

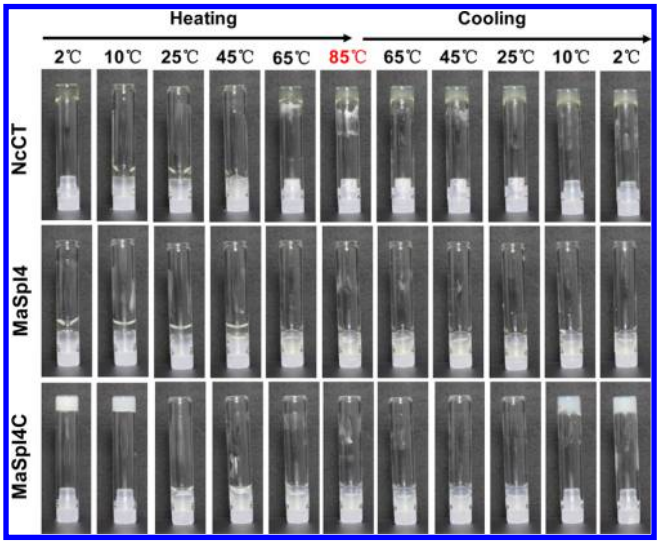

Figure 2. Test of formation of self-supporting hydrogels by NcCT, MaSpI4, and MaSpI4C. Vials containing 15% (w/v) protein solutions were incubated for 10 min at the indicated temperatures and then inverted for image collection.

hydrogel at 2 °C that melted on warming, followed by a switch back to a hydrogel state at 65 °C, and the latter hydrogel did not melt on heating up to 85 °C and subsequent cooling back to 2 °C. When NcCT was genetically fused with the four repetitive units of *N. clavipes* MaSp1, the resulting silk-like protein, MaSpI4C, formed an opaque hydrogel only at low temperatures between 2 and 10 °C. The opaque hydrogel melted upon warming into a solution, which was stably maintained even at a high temperature of 85 °C, and the solution shifted into the hydrogel again on cooling down to 10 °C. As a control, the short repetitive region of silk, MaSpI4, did not form a hydrogel within the wide temperature range tested. The results indicated that the CT of *N. clavipes* MaSp1 was able to form a reversible hydrogel at the low temperature and an irreversible hydrogel at the high temperature, representing gel−sol−gel transitions. In addition, the CT enabled the short repetitive region of silk spidroin to form a reversible hydrogel at low temperatures through genetic fusion of the two spidroin parts.

To confirm and quantify the hydrogel mechanical behavior, the storage (G') and loss (G'') moduli were recorded as a function of temperature using oscillatory rheology (Figure 3). For NcCT, G' (~500 Pa) was greater than G'' at low temperatures, confirming hydrogel formation. NcCT then showed a transition to a liquid state at ~15 °C, followed by a switch back to a hydrogel state at 70 °C, confirming a typical double phase transition. For MaSpI4C, G' (~900 Pa) was found to be approximately an order of magnitude larger than G'' at low temperatures, which confirmed hydrogel formation. MaSpI4C then showed a transition (G' overlapping with G'') between 18 and 21 °C. When the temperature increased further, G' was larger than G'' again, but the differences were lower than 3 pa, which appeared to be not enough to enable the

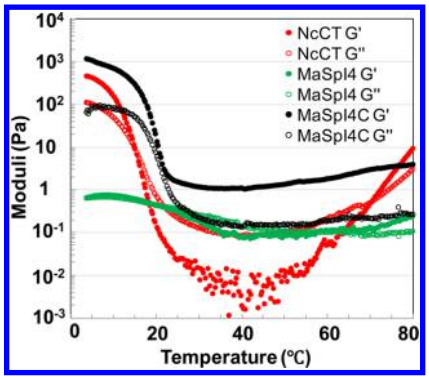

Figure 3. Oscillatory rheology analysis of NcCT, MaSpI4, and MaSpI4C. The concentrations of all samples were 20% (w/v) with a heating rate of 2 °C/min.

formation of a self-supporting hydrogel. As expected, MaSpI4 did not form hydrogels because G' and G'' kept at a very low level within the wide temperature range tested.

To observe the microstructures of the hydrogels, scanning electron microscopy (SEM) was performed on the hydrogel samples following lyophilization, a procedure generally known to have a minimal impact on the structure of hydrogels.[37] The NcCT and MaSpI4C hydrogels formed at 4 °C showed typical porous structures, while the NcCT hydrogel at 65 °C revealed sheet-like morphologies (Figure 4). An interconnected network structure without obvious particles or fibrils was detected, indicating that the hydrogels may be formed through physical cross-linking. In addition, the MaSpI4C hydrogel displayed denser structures than the NcCT hydrogels formed at either 4 or 65 °C, which coincided with its higher mechanical strength as observed from the oscillatory rheology analysis. These results indicated that incorporation of the repeating units of silk spidroin to the CT was beneficial for improving the mechanical properties of the resulting hydrogels.

Temperature-Induced Conformational Changes. To test the effect of temperature on the structures of the recombinant proteins, we used far-UV circular dichroism (CD) spectroscopy to monitor changes in the secondary structures of NcCT, MaSpI4, and MaSpI4C (Figure 5). For NcCT, a typical α-helical pattern with pronounced double minima at 208 and 222 nm was observed at temperatures between 2 and 25 °C. Upon heating to 65 and 85 °C, NcCT showed spectra similar to those at lower temperatures, but with a global lower amplitude and a slight blue shift of the 208 nm minimum to 206 nm. A decrease of the spectrum amplitude suggested that the α-helical structures became looser due to a weakening of the intramolecular interactions upon heating to high temperatures. The blue shift might indicate slight structural changes such as the formation of type I β-turns or disordered structures. We also monitored the ratio of ellipicities at 208 and 222 nm to interpret both helical content and helical arrangements as a ratio of ≤1 was consistent with α-helical coil−coiled arrangement, while a ratio of >1 correlated with single helix. For NcCT, the ratio of ellipicities at 208 and 222 nm was approximately 1.1 at low temperatures and increased to 1.3−1.4 at high temperatures, confirming that the single helix structures were partially unfolded upon heating. These observations were in good agreement with a previous study on CD spectra of another CT construct of *N. clavipes* MaSp1 upon heat and low pH treatments, in which a state of molten globule was proposed for the CT at pH 5.0 and below.[11]

DOI: 10.1021/acs.biomac.5b01231
Biomacromolecules 2015, 16, 3704−3711

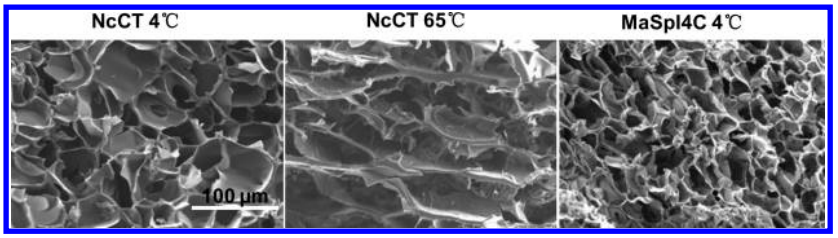

Figure 4. Scanning electron microscopy (SEM) of lyophilized NcCT hydrogels formed at 4 and 65 °C, and the MaSpI4C hydrogel formed at 4 °C.

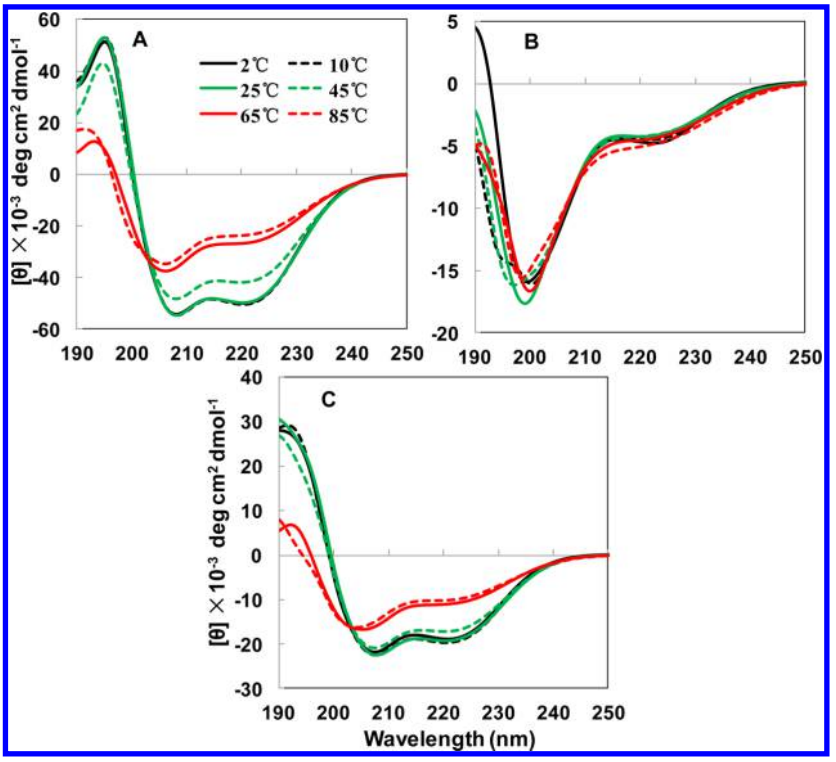

Figure 5. Far-UV CD spectra of NcCT (A), MaSpI4 (B), and MaSpI4C (C) in 20 mM phosphate buffer (pH 7.2) at different temperatures.

MaSpI4C displayed similar structural changes with those of NcCT upon heating, implying that the CT dominated the temperature-dependent conformational changes, whereas MaSpI4 showed a typical random coil structure between 2 and 85 °C. In addition, it can be deduced that the hydrogels of NcCT and MaSpI4C formed at low temperatures did not involve secondary structural changes of the proteins, whereas the NcCT hydrogel at high temperature was related with partial unfolding of the protein secondary structure. Notably, MaSpI4C did not gel at high temperature even though its protein secondary structure was also partially unfolded upon heating. This might be due to the fact that the existence of the four repetitive units in MaSpI4C interfered with physical cross-linking of the CT, which would otherwise lead to hydrogel formation at high temperature. However, the detailed mechanisms remain yet to be explored in the future.

To further examine the possible conformational changes of the recombinant proteins with temperature, fluorescence spectroscopy of 8-anilinonaphthalene-1-sulfonic acid (ANS) was performed to assess surface exposure of hydrophobic amino acids of the proteins (Figure 6). ANS is essentially nonfluorescent in water and becoming appreciably fluorescent when bound to the surface-exposed hydrophobic regions of a protein. This property makes ANS a sensitive indicator of conformational changes and self-assembly of protein polymers.[11] The effect of temperature on ANS fluorescence emission should be excluded as indicated previously.[38] In the temperature range tested, the ANS fluorescence intensity with NcCT was much higher than that with MaSpI4, suggesting that

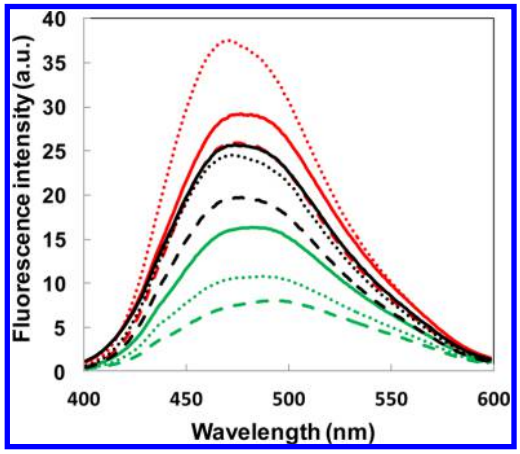

Figure 6. Fluorescence emission spectra of 80 μM ANS in the presence of NcCT (red lines), MaSpI4 (green lines), or MaSpI4C (black lines) when incubated at 4 °C (dotted lines), 25 °C (dash lines), or 65 °C (solid lines).

DOI: 10.1021/acs.biomac.5b01231
Biomacromolecules 2015, 16, 3704−3711

CT was more hydrophobic than the short repetitive units of silk. The signal intensity with NcCT at 65 °C was significantly higher than that at 25 °C. This result implied that NcCT exposed more hydrophobic patches at the high gelation temperature, consistent with the CD result of partial unfolding of the protein at temperatures above 45 °C (Figure 5A). Strikingly, NcCT at 4 °C had even higher affinity for ANS since the signal intensity was increased and shifted toward a lower wavelength of around 471 nm, reflecting stronger hydrophobic interactions that might be involved in the gelation at the low temperature. As for MaSpI4C, higher signal intensity was also seen at 4 and 65 °C, compared to that at 25 °C. Collectively, these data demonstrated that temperature played an important role on the conformational changes of the recombinant silk proteins.

Temperature-Induced Morphological Changes. To investigate self-assembly of the recombinant proteins in solution, atomic force microscopy (AFM) was performed to study the morphologies of NcCT in the phosphate buffer at 4 and 65 °C, the temperatures at which this recombinant protein formed hydrogels (Figure 2). As shown in Figure 7, for NcCT

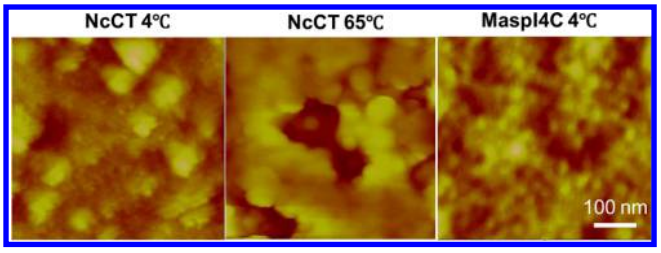

Figure 7. Representative AFM images of the nanostructures derived from self-assembly of NcCT and MaSpI4C in aqueous solutions at 4 or 65 °C.

at 4 °C, some large particles with diameters of about 50−100 nm were observed among smaller particles with diameters less than 10 nm. It appeared that the large particles were formed from the coalescence of the small particles. However, such small particles were barely observed for the same protein at 65 °C. Instead, particles with diameters of about 30−70 nm were formed and appeared to be closely connected, which might be due to physical cross-linking between the exposed hydropobic patches because of partial unfolding of the protein upon heating. AFM analysis of MaSpI4C was also performed at 4 °C because gelation of this protein only occurred at the low temperatures between 2 and 10 °C (Figure 2). Compared to NcCT at 4 °C, MaSpI4C formed uniform particles with diameters of ∼20 nm, which did not aggregate into larger ones but were physically connected. This difference might be due to the existence of the four repetitive units of silk that might physically link each other. These results indicated that self-assembly of the recombinant proteins into nanoglobules of different sizes might be involved in the gelation processes. An earlier study has proposed the important role of nanoglobules as the basic microstructural blocks of silkworm and spider silk fibers.[39] In this context, characterization of the similarities and differences in the microstructures of the above proteins at nanometer scale may help in understandig the detailed gelation mechanisms at low and high temperatures.

Hydrogel Formation Is Conserved with Spider Silk CT. As the nonrepetitive CTs are evolutionarily conserved within spidroins of different spider species,[4] we next examined whether the ability to form hydrogels at dual temperatures was conserved. To this end, we constructed another two plasmids for recombinant expression of the CTs of *A. diadematus* fibroin 3 and *E. australis* MaSp1. The two domains, designated as AdCT and EaCT, share 83.6% and 65.2% identity with NcCT, respectively, based on the online SIM Alignment Tool for protein sequences (http://web.expasy.org/sim/).

As shown in Figure 8, AdCT and EaCT both formed self-supporting hydrogels at 2 and 65 °C. Formation of the

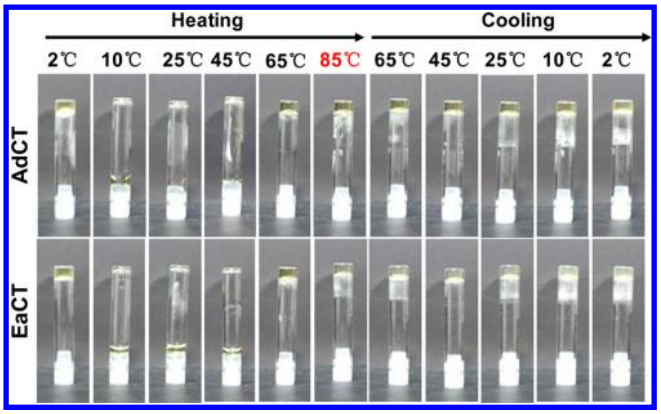

Figure 8. Formation of self-supporting hydrogels by the C-terminal domains of spider *Araneus diadematus* fibroin 3 (AdCT) and *Euprosthenops australis* MaSp1 (EaCT). Vials containing 15% (w/v) protein solutions were incubated for 10 min at the indicated temperatures and then inverted for image collection.

hydrogel at 2 °C was reversible, whereas gelation at 65 °C was irreversible, two characteristics consistent with those of NcCT. Formation of the hydrogels from the conserved CT should be related to its unique structures. Previous studies have revealed that the structure of the CT is a protein fold composed of a parallel-oriented dimeric five-helix bundle.[7] The native fold of the protein hides its hydrophobic residues in a core ensuring protein solubilization through exposed hydrophilic residues. Upon low pH or high temperature treatments, the hydrophobic amino acids are exposed leading to protein aggregation for silk self-assembly. Based on the reported protein structure and the experimental observations described above, here we propose that the hydrogel formation at low temperature was mainly caused by the strengthening of hydrogen bonding and hydrophobic interaction between folded protein molecules. The hydrogen bonds at low temperatures were broken gradually upon warming and the protein experiences a gel-to-solution transition. As the temperature increases further, the protein is partially unfolded and the exposed hydrophobic residues are cross-linked to form an irreversible hydrogel (Figure 9).

CONCLUSIONS

In summary, we have for the first time reported that the conserved CT of spider dragline silk formed dual thermosensitive hydrogels. Gelation at low temperature was reversible, a process mainly driven by hydrogen bonding and hydrophobic interactions between the globular structures of the protein. On the other hand, gelation at high temperature was irreversible and proposed as a process mainly driven by hydrophobic interactions between the partially unfolded protein molecules. In addition, the CT could enable the short repetitive units of silk to gelate at low temperature. It was hypothesized that the

DOI: 10.1021/acs.biomac.5b01231
Biomacromolecules 2015, 16, 3704−3711

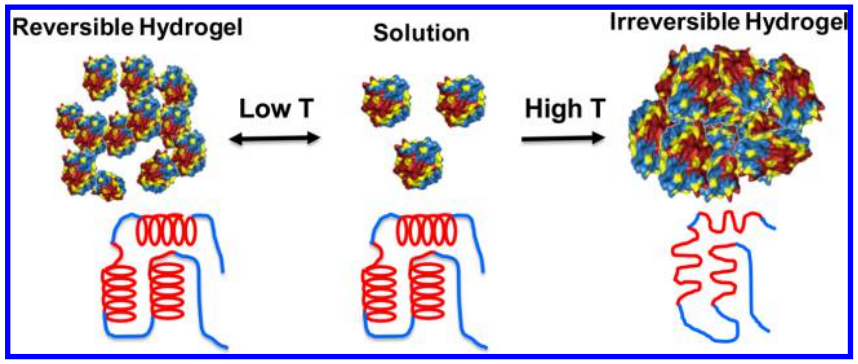

Figure 9. Self-assembly of the conserved spidroin C-terminal domain that leads to the formation of dual thermosensitive hydrogels, one reversible at low temperatures and the other irreversible at high temperatures.

repetitive units in MaSpI4C might interact with each other through hydrogen bonding resulting in higher hydrogel cross-linking density and thus superior mechanical properties when compared with the hydrogel formed at the same temperature with NcCT alone. This study explored the underlying mechanism of gelation for the conserved CT and provided important building blocks for *de novo* design of new protein polymers that may turn into hydrogels with tunable dual thermosensitivity. The newly developed hydrogels herein may be potentially useful for controlled drug delivery and biomedical engineering in the future.

■ ASSOCIATED CONTENT

Supporting Information

The Supporting Information is available free of charge on the ACS Publications website at DOI: 10.1021/acs.biomac.5b01231.

Mass spectroscopy analysis of the purified recombinant silk proteins (Figure S1) (PDF)

■ AUTHOR INFORMATION

Corresponding Author

*E-mail: xiaoxiaxia@sjtu.edu.cn.

Author Contributions

†These authors contributed equally to this work.

Notes

The authors declare no competing financial interest.

■ ACKNOWLEDGMENTS

This study was supported by the National Natural Science Foundation of China (Grant No. 31470216) and the Shanghai Pujiang Program (Grant No. 14PJ1405200 to Z.-G.Q). X.-X.X is grateful to the Program for Professor of Special Appointment (Eastern Scholar) at Shanghai Institutions of Higher Learning (ZXDF080005). The authors would like to thank Instrumental Analysis Center of Shanghai Jiao Tong University (SJTU) for allowing us to use the AFM, SEM, and CD equipment. We also thank Mr. Zhaowen Wang for excellent assistance with initial experiments.

■ REFERENCES

(1) Xu, M.; Lewis, R. V. *Proc. Natl. Acad. Sci. U. S. A.* **1990**, *87*, 7120−7124.
(2) Hinman, M. B.; Lewis, R. V. *J. Biol. Chem.* **1992**, *267*, 19320−19324.
(3) Heim, M.; Keerl, D.; Scheibel, T. *Angew. Chem., Int. Ed.* **2009**, *48*, 3584−3596.
(4) Rising, A.; Johansson, J. *Nat. Chem. Biol.* **2015**, *11*, 309−315.
(5) Gatesy, J.; Hayashi, C.; Motriuk, D.; Woods, J.; Lewis, R. *Science* **2001**, *291*, 2603−2605.
(6) Challis, R. J.; Goodacre, S. L.; Hewitt, G. M. *Insect Mol. Biol.* **2006**, *15*, 45−56.
(7) Hagn, F.; Eisoldt, L.; Hardy, J. G.; Vendrely, C.; Coles, M.; Scheibel, T.; Kessler, H. *Nature* **2010**, *465*, 239−242.
(8) Askarieh, G.; Hedhammar, M.; Nordling, K.; Saenz, A.; Casals, C.; Rising, A.; Johansson, J.; Knight, S. D. *Nature* **2010**, *465*, 236−238.
(9) Hedhammar, M.; Rising, A.; Grip, S.; Martinez, A. S.; Nordling, K.; Casals, C.; Stark, M.; Johansson, J. *Biochemistry* **2008**, *47*, 3407−3417.
(10) Sponner, A.; Vater, W.; Rommerskirch, W.; Vollrath, F.; Unger, E.; Grosse, F.; Weisshart, K. *Biochem. Biophys. Res. Commun.* **2005**, *338*, 897−902.
(11) Gauthier, M.; Leclerc, J.; Lefèvre, T.; Gagné, S. M.; Auger, M. *Biomacromolecules* **2014**, *15*, 4447−4454.
(12) Exler, J. H.; Hümmerich, D.; Scheibel, T. *Angew. Chem., Int. Ed.* **2007**, *46*, 3559−3562.
(13) Ittah, S.; Cohen, S.; Garty, S.; Cohn, D.; Gat, U. *Biomacromolecules* **2006**, *7*, 1790−1795.
(14) Rammensee, S.; Slotta, U.; Scheibel, T.; Bausch, A. R. *Proc. Natl. Acad. Sci. U. S. A.* **2008**, *105*, 6590−6595.
(15) Wang, C.; Stewart, R. J.; Kopecek, J. *Nature* **1999**, *397*, 417−420.
(16) Kopeček, J.; Yang, J. *Angew. Chem., Int. Ed.* **2012**, *51*, 7396−7417.
(17) Cobo, I.; Li, M.; Sumerlin, B. S.; Perrier, S. *Nat. Mater.* **2015**, *14*, 143−159.
(18) Schacht, K.; Scheibel, T. *Curr. Opin. Biotechnol.* **2014**, *29*, 62−69.
(19) Grove, T. Z.; Regan, L. *Curr. Opin. Struct. Biol.* **2012**, *22*, 451−456.
(20) Chilkoti, A.; Christensen, T.; MacKay, J. A. *Curr. Opin. Chem. Biol.* **2006**, *10*, 652−657.
(21) Kurzbach, D.; Hassouneh, W.; McDaniel, J. R.; Jaumann, E. A.; Chilkoti, A.; Hinderberger, D. *J. Am. Chem. Soc.* **2013**, *135*, 11299−11308.
(22) Wang, Q.; Xia, X.; Huang, W.; Lin, Y.; Xu, Q.; Kaplan, D. L. *Adv. Funct. Mater.* **2014**, *24*, 4303−4310.
(23) Truong, M. Y.; Dutta, N. K.; Choudhury, N. R.; Kim, M.; Elvin, C. M.; Hill, A. J.; Thierry, B.; Vasilev, K. *Biomaterials* **2010**, *31*, 4434−4446.
(24) Dutta, N. K.; Truong, M. Y.; Mayavan, S.; Choudhury, N. R.; Elvin, C. M.; Kim, M.; Knott, R.; Nairn, K. M.; Hill, A. J. *Angew. Chem., Int. Ed.* **2011**, *50*, 4428−4431.
(25) Banwell, E. F.; Abelardo, E. S.; Adams, D. J.; Birchall, M. A.; Corrigan, A.; Donald, A. M.; Kirkland, M.; Serpell, L. C.; Butler, M. F.; Woolfson, D. N. *Nat. Mater.* **2009**, *8*, 596−600.
(26) Fang, J.; Zhang, X.; Cai, Y.; Wei, Y. *Biomacromolecules* **2011**, *12*, 1578−1584.

DOI: 10.1021/acs.biomac.5b01231
Biomacromolecules 2015, 16, 3704−3711

(27) Mehl, A. F.; Feer, S. P.; Cusimano, J. S. *Biomacromolecules* **2012**, *13*, 1244−1249.
(28) Li, W.; Huang, L.; Ying, X.; Jian, Y.; Hong, Y.; Hu, F.; Du, Y. *Angew. Chem., Int. Ed.* **2015**, *54*, 3126−3131.
(29) Liu, Y.; Liu, X.; Wu, Y.; Sun, B.; Zhu, M.; Takafuji, M.; Ihara, H. *Chem. Commun.* **2010**, *46*, 430−432.
(30) Seuring, J.; Agarwal, S. *Macromol. Rapid Commun.* **2012**, *33*, 1898−1920.
(31) Xia, M.; Cheng, Y.; Meng, Z.; Jiang, X.; Chen, Z.; Theato, P.; Zhu, M. *Macromol. Rapid Commun.* **2015**, *36*, 477−482.
(32) Käfer, F.; Liu, F.; Stahlschmidt, U.; Jérôme, V.; Freitag, R.; Karg, M.; Agarwal, S. *Langmuir* **2015**, *31*, 8940−8946.
(33) Su, R. S.; Renner, J. N.; Liu, J. C. *Biomacromolecules* **2013**, *14*, 4301−4308.
(34) Gaines, W. A., IV; Marcotte, W. R., Jr *Insect Mol. Biol.* **2008**, *17*, 465−474.
(35) Xia, X. X.; Xu, Q.; Hu, X.; Qin, G.; Kaplan, D. L. *Biomacromolecules* **2011**, *12*, 3844−3850.
(36) Xia, X. X.; Wang, M.; Lin, Y.; Xu, Q.; Kaplan, D. L. *Biomacromolecules* **2014**, *15*, 908−914.
(37) Schacht, K.; Scheibel, T. *Biomacromolecules* **2011**, *12*, 2488−2495.
(38) Poklar, N.; Lah, J.; Salobir, M.; Maček, P.; Vesnaver, G. *Biochemistry* **1997**, *36*, 14345−14352.
(39) Pérez-Rigueiro, J.; Elices, M.; Plaza, G. R.; Guinea, G. V. *Macromolecules* **2007**, *40*, 5360−5365.

DOI: 10.1021/acs.biomac.5b01231
Biomacromolecules 2015, 16, 3704−3711